

Turn Off–On Fluorescent CO₂ Gas Detection Based on Amine-Functionalized Imidazole-Based Poly(ionic liquid)

Seong-Soo Lee,[§] Mirkomil Sharipov,[§] Won June Kim, and Yong-Ill Lee*Cite This: *ACS Omega* 2022, 7, 40485–40492

Read Online

ACCESS |



Metrics & More

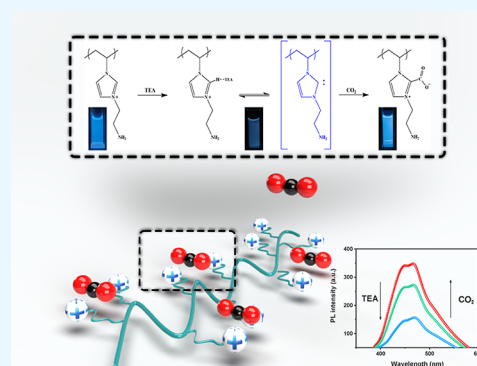


Article Recommendations



Supporting Information

ABSTRACT: Poly(ionic liquids) (PILs) have been widely used for CO₂ capture because their characteristics resemble those of an ionic liquid, yet they have properties typically associated with polymers. We studied the application of the amine-functionalized poly(vinylimidazole)-based PIL (PVIm-NH₂) as a chemosensor. The PVIm-NH₂ was successfully prepared by a facile and low-cost method and was characterized by several analytical techniques: proton nuclear magnetic resonance (¹H NMR), Fourier transform infrared (FT-IR) spectroscopy, gel permeation chromatography (GPC), and spectrofluorometry. The ability of PVIm-NH₂ to detect CO₂ gas was evaluated in the presence of triethylamine (TEA). Under optimized conditions, the detection limit was calculated to be 2.86×10^{-3} M with $R^2 = 0.9906$. Moreover, theoretical and experimental studies suggested a plausible mechanism whereby PVIm-NH₂ generates *N*-heterocyclic carbenes (NHCs) in the presence of TEA, which further reacts with CO₂ gas in aqueous media to form a carboxylic acid. Analysis of PVIm-NH₂ before and after the addition of TEA using the ¹H NMR technique showed the disappearance of the proton peak, thus suggesting a successful generation of NHC. Further analysis via ¹³C NMR revealed the reaction of CO₂ and NHC to form a carboxylic acid group. Finally, we demonstrated that PIL is a promising candidate as a chemosensor through diverse structural modifications.



1. INTRODUCTION

During aerobic respiration, the molecular oxygen (O₂) present in the air is used as the final electron acceptor to generate energy to sustain fundamental life. As a result of the respiration process, exhaled gas contains a high concentration of carbon dioxide (CO₂), a colorless, odorless, and nonflammable gas.¹ The accumulation of exhaled CO₂ in and the resulting oversaturation of poorly ventilated places such as transportation, offices, and factories directly affect people's health and induce physical fatigue. Previous research found that high levels (>5000 ppm) of CO₂ have deleterious effects on human health.^{2–4}

During the last decades, many research groups have shown great interest in developing novel platforms for adsorption and sensing of CO₂.^{5–9} Among various methods, nondispersive infrared (NDIR) spectroscopy is extensively used for measuring the concentration of CO₂ in the air,^{10–12} whereas electrochemical methods are commonly used to measure the concentration of CO₂ dissolved in aqueous solutions.^{13–16} For instance, recently, urea biosensor was developed on the basis of a CO₂ microsensor.¹⁷ However, these approaches are expensive, time- and energy-consuming, and require well-trained personnel. On the other hand, optical CO₂ sensing systems based on fluorescence and UV–vis spectroscopy techniques are more advantageous from the point of view of simplicity, cost-efficiency, and operating conditions.^{18,19} However, the selectivity of optical chemosensors based on

pH shift caused by the hydration of CO₂ to carbonic acid still remains low.^{19–24}

A liquid phase ensures the absorption and sequestration of gases, which are difficult to achieve in the solid and gas phases. Thus, the development of a gas detection method for a liquid phase is ideal for preventing the simultaneous loss of the targeted analyte and for granting subsequent accurate quantitative analysis. From this point of view, poly(ionic liquids) (PILs) have attracted much attention for gas capture and separation applications owing to their unique properties such as their negligible vapor pressure, high ionic conductivity, nonflammability, good thermal stability, and excellent gas selectivity. Moreover, the combination of these properties with the characteristic properties of polymers, including their mechanical stability and chemical tunability, ensures that they have the required multifunctionality.^{25–28} Imidazolium-type PILs demonstrate a greater affinity for CO₂ owing to the CO₂-binding activity of H-2 of the imidazolium ring.²⁹ Among the imidazolium PILs, vinylimidazolium-based PILs have been

Received: September 2, 2022

Accepted: October 17, 2022

Published: October 27, 2022



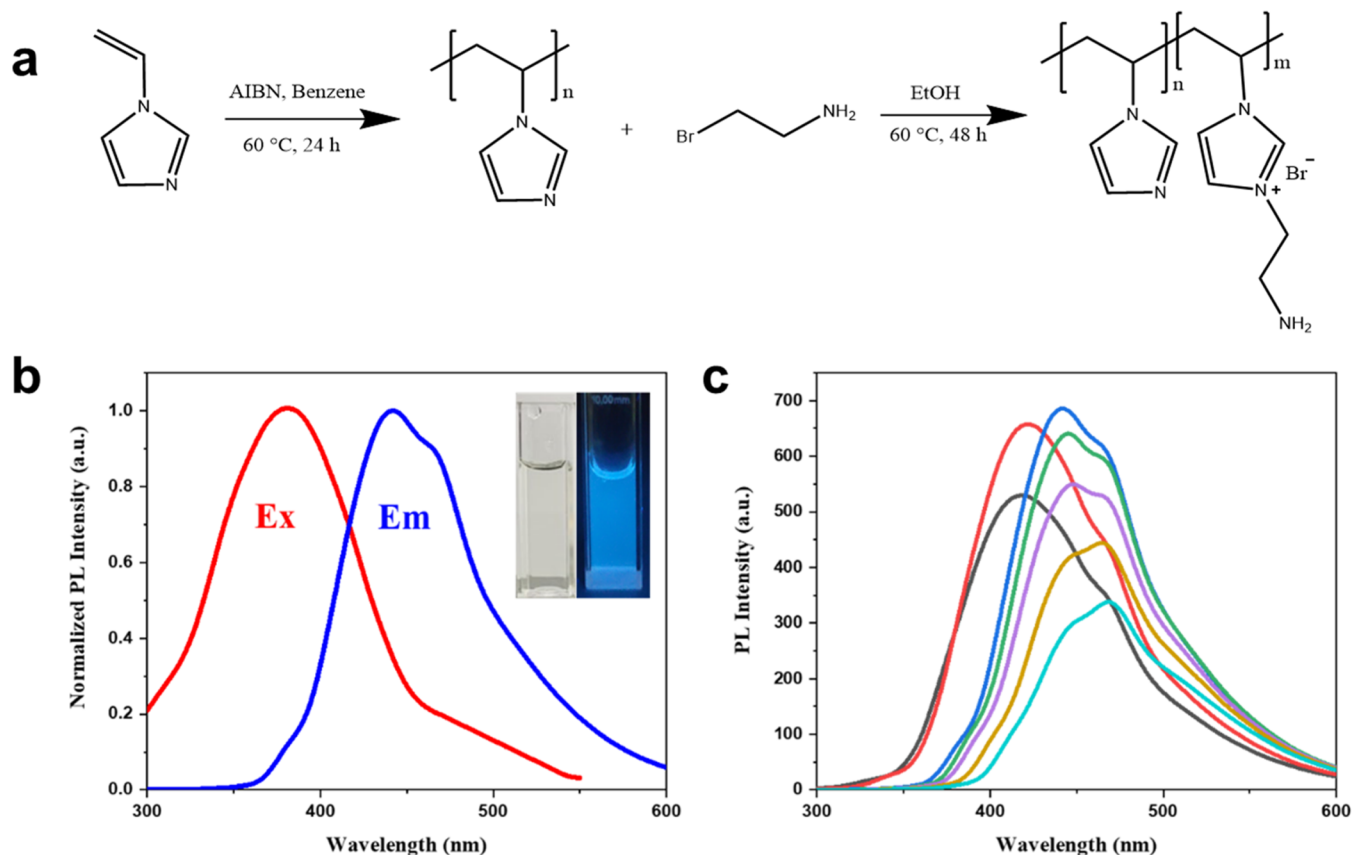


Figure 1. (a) Schematic illustration of the synthetic pathway to form PVIm-NH₂. (b) Fluorescence excitation ($\lambda_{\text{ex}} = 380$ nm) and emission ($\lambda_{\text{em}} = 465$ nm) spectra of an aqueous solution of 0.5 wt % PVIm-NH₂; inset: images of the PVIm-NH₂ aqueous solution taken under visible light (left) and 365 nm UV light (right). (c) Fluorescence emission spectra of the aqueous solution of PVIm-NH₂ at different excitation wavelengths (330–410 nm).

deemed a significant class of PILs because of the plethora of functional replacements available.³⁰ In addition, imidazolium-based PILs can be converted to *N*-heterocyclic carbenes (NHCs) via deprotonation in the presence of a base, thus allowing them to react with CO₂ and generate imidazolium carboxylates.³¹ Despite their high affinity for CO₂, imidazolium PILs have rarely been used for optical CO₂ detection, presumably because the reaction conditions need to be precisely controlled, rendering these PILs unsuitable as chemosensors.

Although numerous chemosensors for CO₂ gas have been developed, most have low solubility or are immiscible with water, compromising their widespread application. Moreover, most reported chemosensors have complicated synthesis pathways and require expensive chemicals. For instance, Liu et al.²¹ and Jang et al.³² reported the preparation of fluorescent chemosensors based on aggregation-induced emission (AIE) for the detection of CO₂ in organic solvents. Yoon's group recently demonstrated that fluorescent probes based on naphthoimidazolium could be used as CO₂ chemosensors in the presence of F⁻ and CN⁻.¹⁹ Another study reported by Yoon's group involved the development of a fluorescent CO₂ chemosensor based on a benzobisimidazolium salt. They exploited the fluoride-induced production of NHC intermediates.²²

Based on the limits and constraints associated with existing PILs, we developed a novel water-soluble and low-cost PIL chemosensor based on imidazolium for sensing CO₂ gas in an

aqueous solution at room temperature. As illustrated in Figure 1a, poly(1-vinylimidazole) (PVIm) was alkylated with bromoethylamine (BEA) to form PVIm-Et-NH₂ (PVIm-NH₂), which is capable of generating an NHC intermediate under basic conditions. The fluorescent CO₂ detection system based on PVIm-NH₂ was designed for use in aqueous media and offers a low detection limit and rapid response times. Furthermore, the mechanism of CO₂ detection was investigated by conducting experimental and theoretical studies.

2. RESULTS AND DISCUSSION

2.1. Characterization of PVIm-NH₂. The chemical structure of PVIm-NH₂ was characterized by Fourier transform infrared (FT-IR), ¹H NMR, and GPC. As shown in Figure S1, the FT-IR spectra of PVIm (top) and PVIm-NH₂ (bottom) demonstrate that the polymerization of PVIm and alkylation of PVIm with Et-NH₂ were successfully accomplished. The spectra of both of these compounds contain peaks attributed to the stretching vibrations of the imidazole rings at 1500.34, 1418.38, 1286.28, and 1230.36 cm⁻¹ (PVIm) and 1496.49, 1418.38, 1285.32, and 1229.39 cm⁻¹ (PVIm-NH₂), respectively. Moreover, the peaks attributed to the stretching vibrations of theazole C–H of PVIm and PVIm-NH₂ appear at 1110.79 and 1088.61 cm⁻¹, while the peaks of the bending vibrations of the heterocycles appear at 918.91, 826.34, and 747.28 cm⁻¹ (PVIm) and 921.80, 830.20, and 749.20 cm⁻¹ (PVIm-NH₂).³³ The characteristic peaks of the N–H bending and C–N stretching modes at 1568.80 and 1160.93 cm⁻¹ on

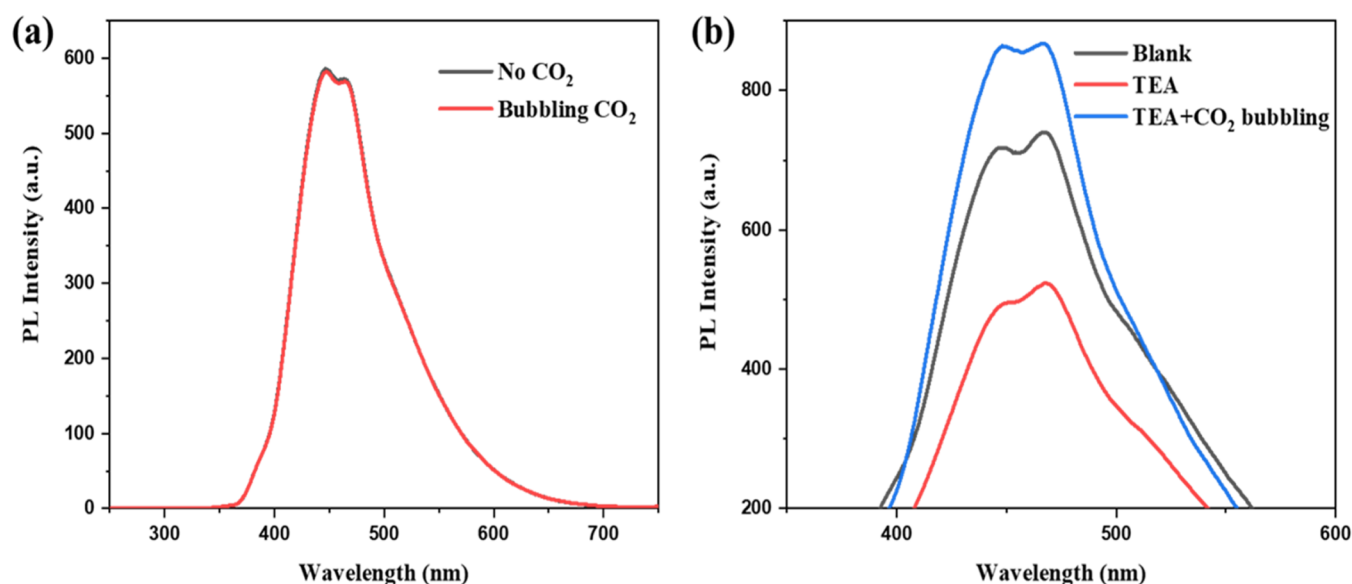


Figure 2. PL spectra of aqueous solutions of (a) 0.5 wt % PVIm-NH₂ and (b) 0.5 wt % PVIm-NH₂ containing TEA (0.32 M) before and after CO₂ gas bubbling at an excitation wavelength of 380 nm (slit with: Ex = 3 nm, Em = 3 nm).

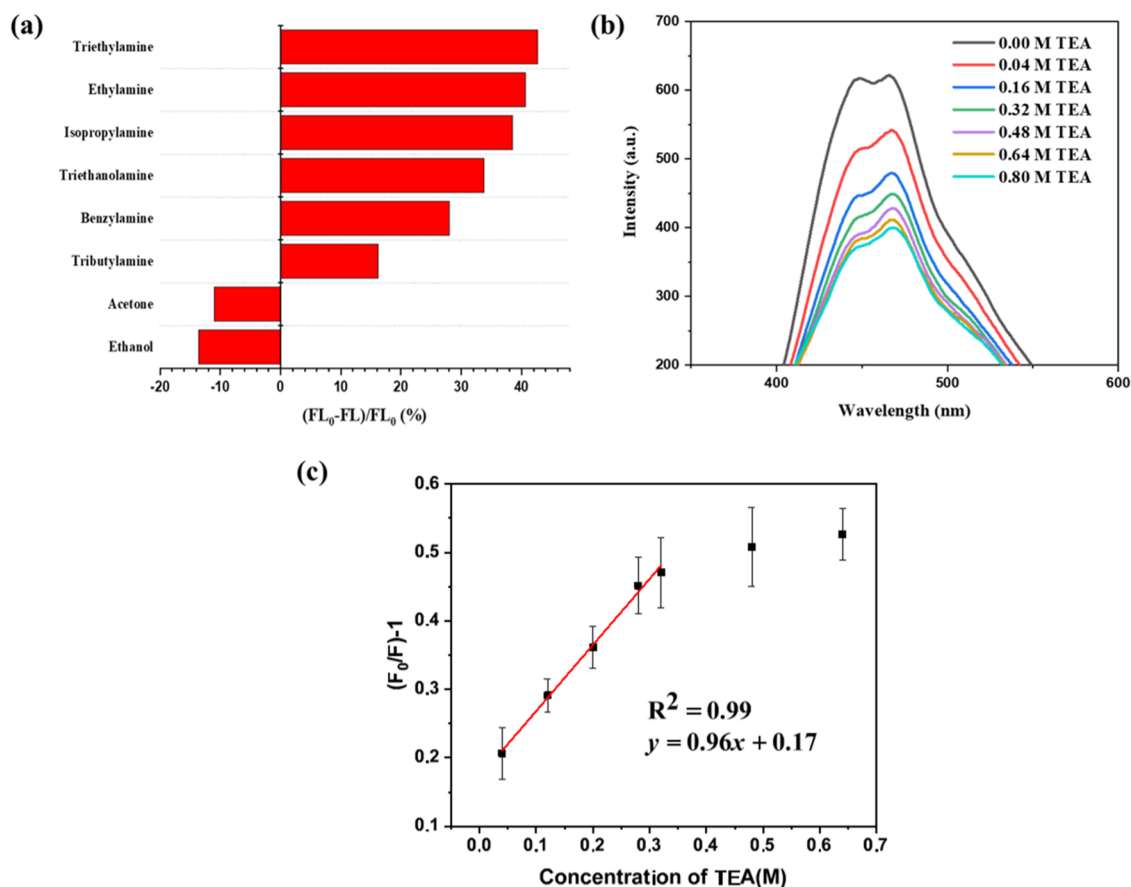


Figure 3. (a) Fluorescence quenching efficiency of amine compounds and alcohol in an aqueous solution containing 0.5% PVIm-NH₂, (b) PL spectra of 0.5 wt % aqueous solutions of PVIm-NH₂ containing various amounts of TEA with 380 nm excitation (slit width: Ex = 3 nm, Em = 3 nm) and (c) plotted against the intensity at 465 nm.

the FT-IR spectrum of PVIm-NH₂ confirm that PVIm has been successfully alkylated to PVIm-NH₂.

The structure of PVIm and its successful alkylation to PVIm-Et-NH₂ were additionally confirmed using ¹H NMR analysis. As shown in Figure S2, the ¹H NMR spectrum of PVIm

exhibits the following characteristic signals: $\delta = 7.42$ – 6.13 ppm (m, 3H, imidazole moiety), $\delta = 3.78$ – 2.31 ppm (m, 1H, methine), and $\delta = 2.22$ – 1.45 ppm (d, 2H, methylene).³⁴ Furthermore, as shown in Figure S3, the characteristic peaks of PVIm-NH₂ appear on the ¹H NMR spectrum of this

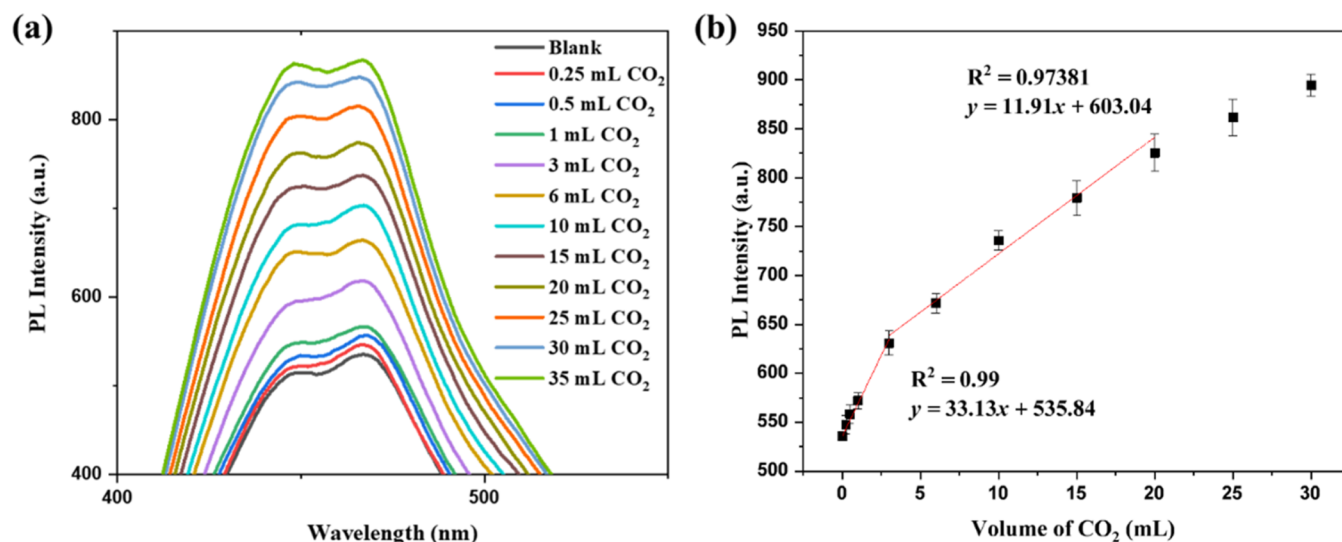


Figure 4. PL spectra of (a) an aqueous solution containing 0.5 wt % PVIm-NH₂ and 0.32 M TEA recorded after bubbling different volumes of CO₂ gas at 380 nm excitation (slit with: Ex = 3 nm, Em = 3 nm) and (b) plotted against the intensity at 465 nm ($n = 3$).

compound: $\delta = 8.30$ – 6.34 ppm (m, 3H, imidazolium moiety), $\delta = 4.58$ – 2.77 ppm (m, 5H, propylene and methine), and $\delta = 2.66$ – 1.63 ppm (s, 2H, methylene).³⁴

The molecular weight of PVIm-NH₂ was determined via GPC analysis using 0.02 N sodium nitrate as the aqueous eluent. The weight-average molecular weight (*M_w*), number-average molecular weight (*M_n*), and polydispersity index (PDI) of PVIm-NH₂ were found to be PVIm-NH₂ 407 878, 346 787, and 1.18, respectively. These results confirm the successful polymerization of PVIm-NH₂.

The prepared PVIm-NH₂ is highly soluble in water because it exists in the form of a salt and also as a result of the abundant amines of the imidazole groups in its backbone, which make it suitable for sensing CO₂ in aqueous media. As presented in Figure 1b, a strong excitation peak is found at 380 nm, and a strong emission peak was recorded at 440 nm with a shoulder at 465 nm. The inset in Figure 1b shows a photographic image of PVIm-NH₂ in an aqueous medium, which, upon exposure to 365 nm UV irradiation, underwent strong blue emission observable by the naked eye. Moreover, as shown in Figure 1c, its emission spectra were measured at different excitation wavelengths ranging from 330 to 410 nm. As the excitation wavelength increased, the representative emission peak was red-shifted. PVIm-NH₂ was observed to exhibit excitation-dependent photoluminescence. As the excitation wavelengths changed from 330 to 380 nm, the emission peak was red-shifted from 418 to 440 nm, and the photoluminescence intensity was enhanced. However, upon exposure to excitation wavelengths above 380 nm, the photoluminescence intensity at 440 nm gradually decreased. This phenomenon was caused by a red edge effect that commonly happens in other imidazolium-based ionic liquids owing to their physical and electrical properties.^{35–37} It occurs primarily because of the spatial heterogeneity of polymeric assemblies, which consist of hydrophilic and hydrophobic pockets that allow multiple solvation sites and contribute to inhomogeneous broadening of the absorption, thus resulting in excitation-dependent PL shift.

2.2. Effect of TEA and CO₂ on the Fluorescence of PVIm-NH₂. Bearing in mind the presence of intrinsic pendant amine, which can act as a base, we have analyzed the fluorescence spectrum of PVIm-NH₂ (5 wt %) bubbled with

CO₂ gas, as illustrated in Figure 2a. The intensity and representative peaks at 440 and 465 nm of PVIm-NH₂ remained unchanged after bubbling CO₂. The nonreactivity of intrinsic pendant amine with imidazolium moiety was also reported in previous work.²⁰ However, as shown in Figure 2b, the addition of TEA strongly quenched the fluorescence—the subsequent addition of CO₂ gas by bubbling again turned on the fluorescence with stronger intensity.

To study the quenching efficiency and selectivity more intensively, a series of 0.5 wt % PVIm-NH₂ aqueous solutions were prepared and mixed with 0.5 v/v% of different amines and alcohol compounds. As shown in Figure 3a, aqueous solutions of the PVIm-NH₂ mixed with various amine compounds display fluorescence quenching under an excitation wavelength of 380 nm. The quenching efficiencies were investigated by calculating the value of $(F_0 - F)/F_0$, where F_0 is the fluorescence intensity of an aqueous solution of PVIm-NH₂ without amine or alcohol and F is the fluorescence intensity of an aqueous solution of PVIm-NH₂ containing amine or alcohol.

Interestingly, all of the amine compounds that were investigated had a quenching effect, whereas acetone and ethanol had the opposite effect, i.e., a slight enhancement. Among the six amine compounds that were tested, TEA had the highest fluorescence quenching efficiency of 42.7%. In comparison, the fluorescence quenching efficiencies of ethylamine, isopropylamine, triethanolamine, benzylamine, and tributylamine were 40.6, 38.5, 33.7, 28.0, and 16.1%, respectively. To evaluate the quenching constants of TEA, aqueous solutions of PVIm-NH₂ were mixed with various amounts of TEA to prepare a range of aqueous solutions with different concentrations of TEA, and the fluorescence intensities were recorded (Figure 3b). The quenching constant of TEA was calculated using the Stern–Volmer equation. According to the Stern–Volmer equation, the quenching constant (K_{sv}) is

$$K_{sv} = (F_0/F - 1)/[\text{quencher}]$$

where F_0 is the fluorescence intensity in the absence of a quencher and F is the fluorescence intensity in the presence of a quencher. As shown in Figure 3c, the K_{sv} of TEA was

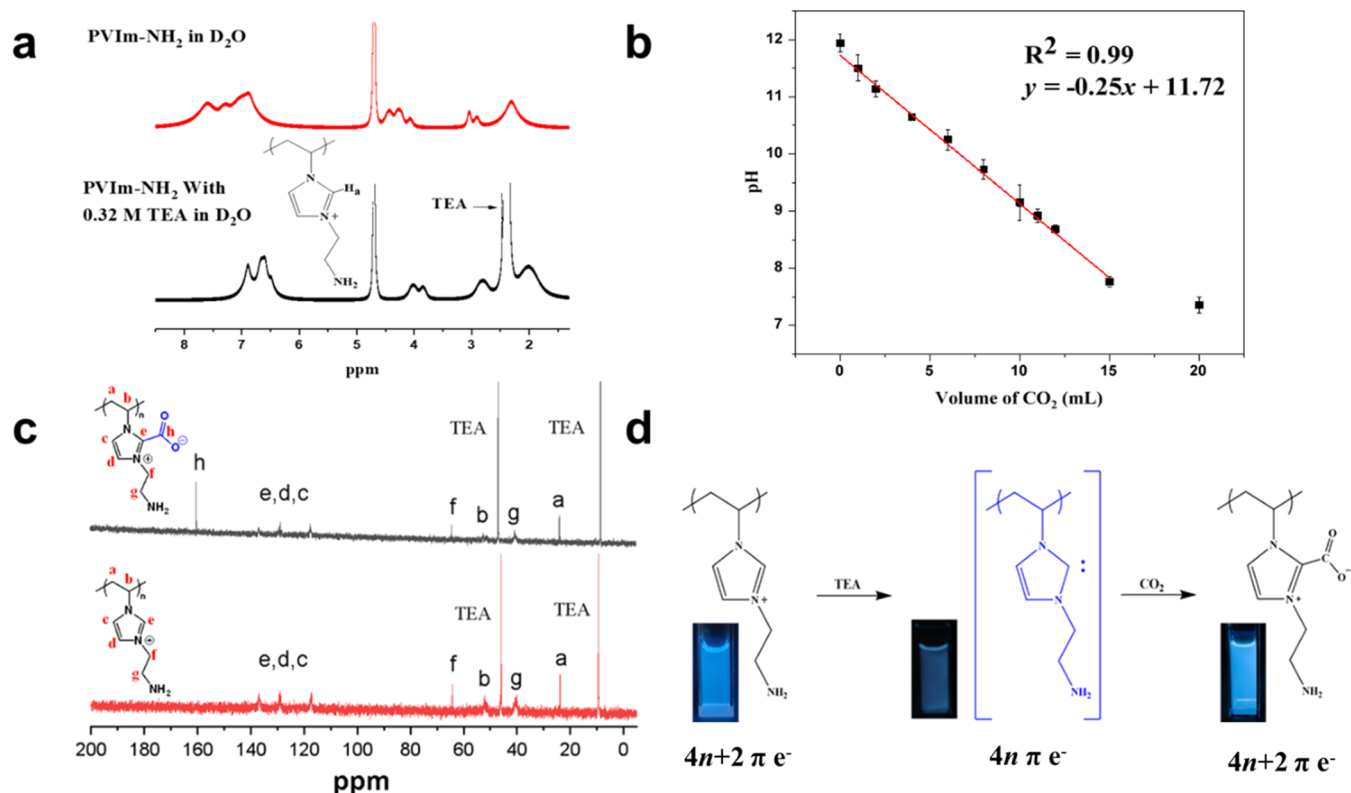


Figure 5. (a) ¹H NMR spectra of PVIA in D₂O and PVIA containing 0.32 M TEA in D₂O, (b) variation in the pH value of an optimized detection solution (0.5 wt % PVIm-NH₂ and 0.32 M TEA in 2 mL DI water) after bubbling different volumes of CO₂ gas, (c) ¹³C NMR spectra of PVIA containing TEA in D₂O and PVIA containing 0.32 M TEA and bubbled CO₂ in D₂O, and (d) schematic illustration of the proposed mechanism for detecting TEA and CO₂. Inset: Fluorescence emission images of samples exposed to 365 nm UV light corresponding to each reaction step.

calculated as 0.9295 with R^2 of 0.9970 for TEA concentrations ranging from 0.04 to 0.32 M. Therefore, to minimize the use of chemicals, the optimal concentration of TEA as quencher was set as 0.32 M because of the relatively weak quenching efficiency at higher concentrations. These results confirmed that triethylamine is the most appropriate compound to enable PVIm-NH₂ to efficiently undergo a structural transformation into NHC.

We have further investigated the effect of solution pH on the quenching efficiency of TEA, as shown in Figure S4. The pH of solutions was manipulated and adjusted by adding HCl or NaOH. As shown in Figure S4b, TEA is not quenching PVIm-NH₂ in a solution with a pH lower than 9 because the pK_a of protonated TEA is 10.75. When the pH of the solution becomes higher than 10, TEA act as a base to deprotonate PVIm-NH₂ and generates NHC.

2.3. Analytical Performance of PVIm-NH₂ for the Detection of CO₂. To evaluate the sensitivity of the developed PVIm-NH₂ PIL toward detecting CO₂, an aqueous solution of 0.5 wt % PVIm-NH₂ containing 0.32 mM TEA in 2 mL of H₂O was prepared at room temperature, after which various volumes of CO₂ were bubbled through the solution. As shown in Figure 4a, the fluorescence intensity of PVIm-NH₂ at 465 nm was gradually enhanced as the amount of CO₂ increased. Noteworthy is that the developed sensing platform showed an immediate response toward CO₂ for volumes as much as 25 mL, beyond which saturation set in. As illustrated in Figure 4b, the fluorescence intensity is linearly related to CO₂ in two distinct ranges: from 0.25 to 3 mL and from 6 to 20 mL with correlation coefficients of 0.991 and 0.974,

respectively. The limit of detection (LOD) was calculated to be 2.86×10^{-3} M (125.87 ppm) using $3\sigma/s$, where “ σ ” and “ s ” are the SD of the blank signals and the slope of the calibration curve, respectively. These results confirmed that the simple and water-soluble PVIm-NH₂ chemosensor we developed was highly sensitive for the detection of CO₂.

2.4. Proposed CO₂ Sensing Mechanism. Supplementary practical and theoretical experiments were conducted to gain insight into the turn off–on mechanism of the sensor we developed for the simultaneous detection of TEA and CO₂, (Figures 5 and 6). First, the generation of NHC in the system was confirmed by comparing the ¹H NMR spectra of PVIA in the presence and absence of TEA. This was accomplished by preparing two solutions of PVIm-NH₂ (0.5 wt %) in D₂O, and TEA was added to one of these solutions such that the final concentration thereof was 0.32 M. Both PVIm-NH₂ solutions were analyzed using ¹H NMR to investigate the structural changes that occurred after adding TEA. As shown in Figure 5a, the apparent difference between the two ¹H NMR spectra was the disappearance of one of three proton peaks recorded in the range 8.30–6.34 ppm and assigned to the imidazolium protons. The disappearance of the proton peak could also be the result of hydrogen–deuterium exchange because of the catalysis of TEA. However, the observed PL quenching and the chemical shift in the upfield direction confirm the removal of the proton (H_a) by TEA. The carbene unit has a higher electron density around its nucleus, which has a shielding effect and induces the peak shift. The CO₂ gas that was subsequently bubbled through the solution resulted in the formation of the carboxylate function and carbonic acid. In addition, the

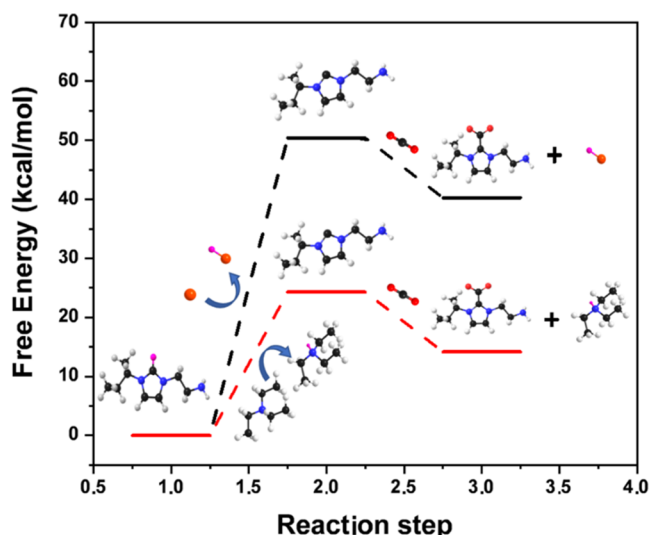


Figure 6. Free energy diagrams of CO₂ capture by PVIm-NH₂ in the absence (black) and presence (red) of TEA.

bubbling CO₂ gas gradually lowers the pH of the solution toward acidic, as presented in Figure 5b. To further confirm the reaction of CO₂ with NHC, ¹³C NMR and FT-IR analyses were conducted. As shown in Figure 5c, a new peak on the ¹³C NMR spectrum at 160 ppm appears after the reaction of PVIm-NH₂ NHC with CO₂, corresponding to carboxylic acid. The ¹³C NMR results were in accordance with other works reported in the literature.³⁸ In addition, the appearance of a new peak located at around 1710 cm⁻¹ on the FT-IR spectrum corresponding to C=O stretching confirms the formation of the carboxylic acid group, as illustrated in Figure 5s.³⁹ The proposed mechanism of generation of NHC by removing the H_a proton, catalysis by TEA, and the subsequent reaction with CO₂ gas explains the observed photophysical changes, as displayed in Figure 5d. The generation of NHC in the presence of TEA is accompanied by a transformation of the aromatic imidazolium ring into an antiaromatic ring with 4n π electrons. Antiaromatic compounds are rich in electrons and unstable compared to aromatic compounds; therefore, their photophysical properties differ. Yoon et al. reported that antiaromatic compounds lack fluorescence and have short lowest excited-state lifetimes, which contrast with aromatic analogs.⁴⁰ The reaction of CO₂ with the NHC group restores the aromaticity of the imidazolium ring, thus resulting in fluorescence recovery.

2.5. DFT Study of the Proposed CO₂ Sensing Mechanism. According to the report by Xu et al., the reaction of CO₂ with amine-functionalized imidazolium PILs generates carbamic acid salts in an aqueous solution.²⁰ However, our proposed mechanism is based on the following: the disappearance of the H_a proton peak from the ¹H NMR spectrum, the apparition of new peak on ¹³C NMR, and the gradual change in the pH value from basic to acidic following the addition of CO₂ indicated that the reaction of PVIm-NH₂ with TEA would generate an NHC group. We performed DFT calculations as an additional confirmation of the proposed mechanism. As shown in Figure 6, the free energies were calculated for two reaction mechanisms: CO₂ capture by PVIm-NH₂ in the (1) absence and (2) presence of TEA. The practical experiments revealed no notable PL changes in the first scenario (Figure 2a). The theoretical calculation of the

free energy of CO₂ capture in the absence of TEA, considering that PVIm-NH₂ exists in the form of a salt with bromide ions, indicated the necessity for high activation energy of 50.408 kcal/mol.

On the other hand, the addition of TEA to PVIm-NH₂ quenched the fluorescence intensity, which subsequently intensified again after CO₂ bubbling. Under these conditions, the calculated free energy required to form NHC was 24.277 kcal/mol, 2-fold lower than that required for the first mechanism. Based on the results we obtained from our practical and theoretical experiments, we confirmed that TEA acts as a catalyst to generate the NHC group, which further reacts with CO₂, thus enabling the formation of the carboxylate functional group.

3. CONCLUSIONS

A novel water-soluble PIL was synthesized using a facile and inexpensive method to develop a PVIm-NH₂ chemosensor for the sensitive detection of CO₂ gas. The PVIm-NH₂ polymer exhibited an immediate response to CO₂ gas via a turn off–on mechanism in the presence of TEA with a good LOD calculated to be 2.86 × 10⁻³ M (125.87 ppm). In the presence of TEA, the imidazolium moiety of PVIm-NH₂ changed to NHC, which resulted in fluorescence quenching. The formed NHC group efficiently reacted with the subsequently added CO₂ gas via bubbling, thus allowing the carboxylation of the imidazolium moiety. As a result of this carboxylation reaction, the formerly quenched fluorescence was restored and its emission intensified, thus demonstrating that this PVIm-NH₂-based PIL is a promising CO₂ sensor. Finally, although TEA exhibited the highest quenching efficiency of all of the amines that were assessed, the sensing platform could be optimized even further for detecting other amine molecules via the formation of NHC. Therefore, we consider the developed PIL to have excellent potential for application as a chemosensor to detect other species by various structural modifications.

4. EXPERIMENTAL SECTION

4.1. Materials. 1-Vinylimidazole and 2-bromoethylamine hydrobromide (98%) were purchased from Alfa Aesar. Benzene (>99.5%) and triethylamine (TEA) were obtained from Dae Jung, Corp (South Korea). Hexanes (extra pure grade) and ethyl alcohol (95%, extra pure grade) were purchased from Duksan, Corp (South Korea). Acetone (99.5%) was obtained from Samchun, Corp (South Korea). All reagents and solvents were used as received without further purification. The distilled water used in all experiments was purified using a Milli-Q water purification system. The resistivity of the water was higher than 18 MΩ·cm⁻¹.

4.2. Equipment and Measurement. Proton nuclear magnetic resonance (¹H NMR) was recorded using a Bruker Avance (400 MHz magnet, Bruker, Germany). Fourier transform infrared (FT-IR) spectra were recorded on an FT/IR-6300 Fourier Transform Infrared Spectrometer (Jasco, Japan). Gel permeation chromatography (GPC) was carried out on a Breeze System (Waters) with a series of four Water Ultrahydrogel columns (Linear, 120, 250, and 500), a Waters 2414 Refractive Index detector, and a Waters 1525 Binary pump; mobile phase: 0.02 N sodium nitrate in water at 30 °C, calibrated with a poly(ethylene glycol) standard to determine the representative molecular weight of PVIm-NH₂. The fluorescence experiments were performed on an FP-6500

spectrofluorometer (Jasco, Japan) using a quartz cuvette with a 1 cm path length.

4.3. Synthesis of PVIm. Poly(1-vinylimidazole) (PVIm) was prepared by a modification of the free radical polymerization method reported previously.³³ Briefly, 9.624 mL (0.106 mol) of 1-vinylimidazole monomer and 100 mg (0.61 mmol) of AIBN were completely dissolved in 96 mL of benzene in a 250 mL three-neck volumetric flask with mild stirring and heating. The mixed solution was heated at 60 °C for 24 h under reflux and nitrogen atmosphere. After the polymerization was complete, the product was precipitated by acetone and then washed three times with acetone and hexane, respectively. The obtained PVIm (light yellow powder) was dried in a vacuum oven at 40 °C for 48 h.

4.4. Synthesis of PVIm-NH₂. PVIm (1 g, 10 mmol; based on the monomer) and 2-bromoethylamine hydrobromide (3.07 g, 15 mmol) were added to 50 mL of ethanol in a molar ratio of 1:1.5, and the mixed solution was sonicated to achieve complete dissolution. The reaction mixture was heated to reflux (60 °C) for 48 h with constant stirring under a nitrogen atmosphere. PVIm-NH₂ was precipitated by adding isopropyl alcohol, washed with hexane, and dried in a vacuum oven at 40 °C for 48 h.

4.5. Assessment of the CO₂ Gas Detection Performance of PVIm-NH₂. PVIm-NH₂ of ~1 w/w% was dissolved in DI water under ultrasonication. Afterward, TEA was dissolved in the PVIm-NH₂ aqueous solution with a final concentration of 0.80 M and stored at room temperature. A syringe (0.457 mm outer diameter) was used to inject increasing volumes of CO₂ into the aqueous solution of PVIm-NH₂ containing TEA. The fluorescence intensity was recorded with a spectrofluorometer (excitation wavelength = 386 nm, slit width: Ex = 3 nm, Em = 3 nm).

4.6. Computational Details. We performed quantum chemical calculations using the NWChem 7.0 package.^{41–43} Density functional theory (DFT) based on the B3LYP hybrid functional was used,^{44,45} and the electronic states were expanded using the def2-TZVPD basis set⁴⁶ for all elements. The Gibbs free energy for all reactants, products, and reaction intermediates at 1 atm and 298.15 K was estimated by calculating their molecular partition functions. The solvation free energies were calculated within the framework of the COSMO method⁴⁷ using a variation thereof known as the solvation model based on the density (SMD).⁴⁸

■ ASSOCIATED CONTENT

SI Supporting Information

The Supporting Information is available free of charge at <https://pubs.acs.org/doi/10.1021/acsomega.2c05695>.

FT-IR spectra of PVIm and PVIm-NH₂ (Figure S1); ¹H NMR spectrum of PVIm (Figure S2); ¹H NMR spectrum of PVIm-NH₂ (Figure S3); effect of pH on quenching efficiency of TEA on PVIm-NH₂ (Figure S4); and FT-IR spectra of PVIm-NH₂ after addition of TEA and after bubbling CO₂ (Figure S5) (PDF)

■ AUTHOR INFORMATION

Corresponding Author

Yong-Ill Lee – Department of Chemistry, Changwon National University, Changwon 51140, Republic of Korea; Faculty of Chemical Engineering, Industrial University of Ho Chi Minh

City, Ho Chi Minh City 71408, Vietnam; orcid.org/0000-0001-5383-9801; Email: yilee@changwon.ac.kr

Authors

Seong-Soo Lee – Department of Chemistry, Changwon National University, Changwon 51140, Republic of Korea
Mirkomil Sharipov – Department of Chemistry, Changwon National University, Changwon 51140, Republic of Korea
Won June Kim – Department of Chemistry, Changwon National University, Changwon 51140, Republic of Korea; orcid.org/0000-0001-6421-9237

Complete contact information is available at:

<https://pubs.acs.org/10.1021/acsomega.2c05695>

Author Contributions

[§]S.-S.L. and M.S. contributed equally to this work.

Notes

The authors declare no competing financial interest.

■ ACKNOWLEDGMENTS

This work was supported by the National Research Foundation of Korea (NRF) grant funded by the Korea government (MSIT) (no. 2020R1A2C2007028).

■ REFERENCES

- (1) Lozano, J.; Suárez, J. I.; Arroyo, P.; Ordiales, J. M.; Alvarez, F. Wireless Sensor Network For Indoor Air Quality Monitoring. *Chem. Eng. Trans.* **2012**, *30*, 319–324.
- (2) Andrew, K. P. Evaluating building IAQ and ventilation with indoor carbon dioxide. *ASHRAE Trans.* **1997**, *103*, 193–204.
- (3) Lipsett, M. J.; Shusterman, D.; Beard, R. Inorganic Compounds of Carbon, Nitrogen, and Oxygen. In *Patty's Industrial Hygiene and Toxicology*; Clayton, G. D.; Clayton, F. D., Eds.; John Wiley & Sons, 1994; pp 4523–4643.
- (4) Yi, S.; Park, Y.; Han, S.; Min, N.; Kim, E.; Ahn, T. Novel NDIR CO₂ Sensor for Indoor Air Quality Monitoring. In Proceedings of 13th International Conference Solid-State Sensors, Actuators and Microsystems, 2005. Digest of Technical Papers. TRANSDUCERS'05. IEEE, 2005; Vol. 2, pp 1211–1214.
- (5) Kanaparthi, S.; Singh, S. G. Chemiresistive sensor based on zinc oxide nanoflakes for CO₂ detection. *ACS Appl. Nano Mater.* **2019**, *2*, 700–706.
- (6) Gaytan, J. N.; Li, Q.; Sanders, L.; Rodrigues, R. R.; Hill, G.; Delcamp, J. H. Pyridyl CO₂ Fixation Enabled by a Secondary Hydrogen Bonding Coordination Sphere. *ACS Omega* **2020**, *5*, 11687–11694.
- (7) Yadav, A. A.; Lokhande, A. C.; Kim, J. H.; Lokhande, C. D. Improvement in CO₂ sensing characteristics using Pd nanoparticles decorated La₂O₃ thin films. *J. Ind. Eng. Chem.* **2017**, *49*, 76–81.
- (8) Akram, M. M.; Nikfarjam, A.; Hajghassem, H.; Ramezannezhad, M.; Iraj, M. Low cost and miniaturized NDIR system for CO₂ detection applications. *Sens. Rev.* **2020**, *40*, 637–646.
- (9) Hussain, S.; Shahid Chatha, S. A.; Hussain, A. I.; Hussain, R.; Mehboob, M. Y.; Gulzar, T.; Mansha, A.; Shahzad, N.; Ayub, K. Designing Novel Zn-Decorated Inorganic B12P12 Nanoclusters with Promising Electronic Properties: A Step Forward toward Efficient CO₂ Sensing Materials. *ACS Omega* **2020**, *5*, 15547–15556.
- (10) Neethirajan, S.; Jayas, D. S.; Sadistap, S. Carbon Dioxide (CO₂) Sensors for the Agri-food Industry—A Review. *Food Bioprocess Technol.* **2009**, *2*, 115–121.
- (11) Yasuda, T.; Yonemura, S.; Tani, A. Comparison of the characteristics of small commercial NDIR CO₂ sensor models and development of a portable CO₂ measurement device. *Sensors* **2012**, *12*, 3641–3655.
- (12) Frodl, R.; Tille, T. A High-Precision NDIR CO₂ Gas Sensor for Automotive Applications. *IEEE Sensors J.* **2006**, *6*, 1697–1705.

- (13) Xie, X.; Bakker, E. Non-Severinghaus potentiometric dissolved CO₂ sensor with improved characteristics. *Anal. Chem.* **2013**, *85*, 1332–1336.
- (14) Decker, M.; Oelßner, W.; Zosel, J. Electrochemical CO₂ Sensors with Liquid or Pasty Electrolyte. *Carbon Dioxide Sens.* **2019**, 87–116.
- (15) Chen, L. D.; Mandal, D.; Pozzi, G.; Gladysz, J. A.; Bühlmann, P. Potentiometric sensors based on fluorinated membranes doped with highly selective ionophores for carbonate. *J. Am. Chem. Soc.* **2011**, *133*, 20869–20877.
- (16) Lee, I.; Akbar, S. A.; Dutta, P. K. High temperature potentiometric carbon dioxide sensor with minimal interference to humidity. *Sens. Actuators, B* **2009**, *142*, 337–341.
- (17) Fapyane, D.; Berillo, D.; Marty, J.-L.; Revsbech, N. P. Urea Biosensor Based on a CO₂ Microsensor. *ACS Omega* **2020**, *5*, 27582–27590.
- (18) Sun, J.; Ye, B.; Xia, G.; Zhao, X.; Wang, H. A colorimetric and fluorescent chemosensor for the highly sensitive detection of CO₂ gas: experiment and DFT calculation. *Sens. Actuators, B* **2016**, *233*, 76–82.
- (19) Kwon, N.; Baek, G.; Swamy, K.; Lee, M.; Xu, Q.; Kim, Y.; Kim, S.-J.; Yoon, J. Naphthoimidazolium based ratiometric fluorescent probes for F⁻ and CN⁻, and anion-activated CO₂ sensing. *Dyes Pigm.* **2019**, *171*, No. 107679.
- (20) Xu, Q.; Lee, S.; Cho, Y.; Kim, M. H.; Bouffard, J.; Yoon, J. Polydiacetylene-based colorimetric and fluorescent chemosensor for the detection of carbon dioxide. *J. Am. Chem. Soc.* **2013**, *135*, 17751–17754.
- (21) Liu, Y.; Tang, Y.; Barashkov, N. N.; Irgibaeva, I. S.; Lam, J. W.; Hu, R.; Birimzhanova, D.; Yu, Y.; Tang, B. Z. Fluorescent chemosensor for detection and quantitation of carbon dioxide gas. *J. Am. Chem. Soc.* **2010**, *132*, 13951–13953.
- (22) Guo, Z.; Song, N. R.; Moon, J. H.; Kim, M.; Jun, E. J.; Choi, J.; Lee, J. Y.; Bielawski, C. W.; Sessler, J. L.; Yoon, J. A benzobisimidazolium-based fluorescent and colorimetric chemosensor for CO₂. *J. Am. Chem. Soc.* **2012**, *134*, 17846–17849.
- (23) Zhu, W.-B.; Wei, T.-b.; Fan, Y.-Q.; Qu, W.-J.; Zhu, W.; Ma, X.-Q.; Yao, H.; Zhang, Y.-M.; Lin, Q. A pillar [5] arene-based and OH⁻-dependent dual-channel supramolecular chemosensor for recyclable CO₂ gas detection: High sensitive and selective off-on-off response. *Dyes Pigm.* **2020**, *174*, No. 108073.
- (24) Gowri, A.; Khamrang, T.; Velusamy, M.; Kathiresan, M.; Kumar, M. D.; Jaccob, M.; Kathiravan, A. Pyrene Based Chemosensor for Carbon Dioxide Gas—Meticulous Investigations and Digital Image based RGB Analysis. *Sens. Actuators Rep.* **2020**, *2*, No. 100007.
- (25) Sang, Y.; Huang, J. Benzimidazole-based hyper-cross-linked poly (ionic liquid) s for efficient CO₂ capture and conversion. *Chem. Eng. J.* **2020**, *385*, No. 123973.
- (26) Mecerreyes, D. Polymeric ionic liquids: Broadening the properties and applications of polyelectrolytes. *Prog. Polym. Sci.* **2011**, *36*, 1629–1648.
- (27) Raja Shahrom, M. S.; Wilfred, C. D.; MacFarlane, D. R.; Vijayraghavan, R.; Chong, F. K. Amino acid based poly (ionic liquid) materials for CO₂ capture: effect of anion. *J. Mol. Liq.* **2019**, *276*, 644–652.
- (28) Bernard, F. L.; Polesso, B. B.; Cobalchini, F. W.; Donato, A. J.; Seferin, M.; Ligabue, R.; Chaban, V. V.; do Nascimento, J. F.; Dalla Vecchia, F.; Einloft, S. CO₂ capture: Tuning cation-anion interaction in urethane based poly (ionic liquids). *Polymer* **2016**, *102*, 199–208.
- (29) Wang, X.; Akhmedov, N. G.; Duan, Y.; Luebke, D.; Hopkinson, D.; Li, B. Amino acid-functionalized ionic liquid solid sorbents for post-combustion carbon capture. *ACS Appl. Mater. Interfaces* **2013**, *5*, 8670–8677.
- (30) Yuan, J.; Mecerreyes, D.; Antonietti, M. Poly (ionic liquid) s: an update. *Prog. Polym. Sci.* **2013**, *38*, 1009–1036.
- (31) Dröge, T.; Glorius, F. The Measure of All Rings—N-Heterocyclic Carbenes. *Angew. Chem., Int. Ed.* **2010**, *49*, 6940–6952.
- (32) Jang, M.; Kang, S.; Han, M. S. A simple turn-on fluorescent chemosensor for CO₂ based on aggregation-induced emission: application as a CO₂ absorbent screening method. *Dyes Pigm.* **2019**, *162*, 978–983.
- (33) Khaligh, N. G. Poly (N-vinylimidazole) as a halogen-free and efficient catalyst for N-Boc protection of amines under solvent-free conditions. *RSC Adv.* **2012**, *2*, 12364–12370.
- (34) Endo, A.; Nagakura, T.; Kawakami, H.; Asayama, S. Synthesis and characterization of lactosylated poly(1-vinylimidazole) for cell-specific plasmid DNA carrier. *Intern. Med. Care* **2020**, *4*, 1–5.
- (35) Guleria, A.; Singh, A. K.; Adhikari, S. Optical properties of irradiated imidazolium based room temperature ionic liquids: new microscopic insights into the radiation induced mutations. *Phys. Chem. Chem. Phys.* **2015**, *17*, 11053–11061.
- (36) Boydston, A. J.; Vu, P. D.; Dykhnou, O. L.; Chang, V.; Wyatt, A. R.; Stockett, A. S.; Ritschdorff, E. T.; Shear, J. B.; Bielawski, C. W. Modular fluorescent benzobis (imidazolium) salts: Syntheses, photophysical analyses, and applications. *J. Am. Chem. Soc.* **2008**, *130*, 3143–3156.
- (37) Mandal, P. K.; Sarkar, M.; Samanta, A. Excitation-Wavelength-Dependent Fluorescence Behavior of Some Dipolar Molecules in Room-Temperature Ionic Liquids. *J. Phys. Chem. A* **2004**, *108*, 9048–9053.
- (38) Pinaud, J.; Vignolle, J.; Gnanou, Y.; Taton, D. Poly(N-heterocyclic-carbene)s and their CO₂ Adducts as Recyclable Polymer-Supported Organocatalysts for Benzoin Condensation and Transesterification Reactions. *Macromolecules* **2011**, *44*, 1900–1908.
- (39) Wang, X.; Wang, D.; Guo, Y.; Yang, C.; Iqbal, A.; Liu, W.; Qin, W.; Yan, D.; Guo, H. Imidazole derivative-functionalized carbon dots: using as a fluorescent probe for detecting water and imaging of live cells. *Dalton Trans.* **2015**, *44*, 5547–5554.
- (40) Yoon, M.-C.; Cho, S.; Suzuki, M.; Osuka, A.; Kim, D. Aromatic versus Antiaromatic Effect on Photophysical Properties of Conformationally Locked trans-Vinylene-Bridged Hexaphyrins. *J. Am. Chem. Soc.* **2009**, *131*, 7360–7367.
- (41) Aprà, E.; Bylaska, E. J.; de Jong, W. A.; Govind, N.; Kowalski, K.; Straatsma, T. P.; Valiev, M.; van Dam, H. J. J.; Alexeev, Y.; Anchell, J.; et al. NWChem: Past, present, and future. *J. Chem. Phys.* **2020**, *152*, No. 184102.
- (42) Kendall, R. A.; Aprà, E.; Bernholdt, D. E.; Bylaska, E. J.; Dupuis, M.; Fann, G. I.; Harrison, R. J.; Ju, J.; Nichols, J. A.; Nieplocha, J.; et al. High performance computational chemistry: An overview of NWChem a distributed parallel application. *Comput. Phys. Commun.* **2000**, *128*, 260–283.
- (43) Valiev, M.; Bylaska, E. J.; Govind, N.; Kowalski, K.; Straatsma, T. P.; Van Dam, H. J. J.; Wang, D.; Nieplocha, J.; Apra, E.; Windus, T. L.; de Jong, W. NWChem: A comprehensive and scalable open-source solution for large scale molecular simulations. *Comput. Phys. Commun.* **2010**, *181*, 1477–1489.
- (44) Becke, A. D. A new mixing of Hartree–Fock and local density-functional theories. *J. Chem. Phys.* **1993**, *98*, 1372–1377. (accessed 2022/02/14).
- (45) Lee, C.; Yang, W.; Parr, R. G. Development of the Colle-Salvetti correlation-energy formula into a functional of the electron density. *Phys. Rev. B* **1988**, *37*, 785–789.
- (46) Rappoport, D.; Furche, F. Property-optimized Gaussian basis sets for molecular response calculations. *J. Chem. Phys.* **2010**, *133*, No. 134105.
- (47) Klamt, A.; Schüürmann, G. COSMO: a new approach to dielectric screening in solvents with explicit expressions for the screening energy and its gradient. *J. Chem. Soc., Perkin trans. 2* **1993**, 799–805.
- (48) Marenich, A. V.; Cramer, C. J.; Truhlar, D. G. Universal Solvation Model Based on Solute Electron Density and on a Continuum Model of the Solvent Defined by the Bulk Dielectric Constant and Atomic Surface Tensions. *J. Phys. Chem. B* **2009**, *113*, 6378–6396.